Improvement of Compton imaging efficiency by using side-neighbor events

Weiyi Wang*, Willy R. Kaye, Jae Cheon Kim, Feng Zhang, Zhong He

Department of Nuclear Engineering and Radiological Sciences, University of Michigan, 2355 Bonisteel Boulevard, Ann Arbor, MI 48109, USA

ARTICLE INFO

ABSTRACT

In a pixelated detector, an electron cloud can be collected by and shared between several adjacent pixels. By including these charge-sharing events, the Compton-imaging efficiency can be improved for 3D position sensitive room-temperature CdZnTe gamma-ray detectors. Simulated photopeak events that trigger three separate pixels with two pixels being adjacent to each other, which are called three-pixel side-neighbor photopeak events, were divided into six categories based on interaction type. Analysis of this simulation shows that the most effective strategy is to treat all side-neighbor events as charge-sharing events and to combine all side-neighbor signals into a single interaction. By including these side-neighbor events in the Compton image reconstruction, we can improve the imaging efficiency by 45% and 160% for 662 keV and 1333 keV incident photons, respectively. The simulation also shows that 76% of these combined events reconstruct to rings that pass the source direction. Measured data is presented to validate the simulation results.

1. Introduction

Traditional spectroscopic gamma-ray detectors record the total energy deposited by each gamma ray in the active volume, producing a single energy spectrum. However, when the three-dimensional interaction positions of each gamma ray can be recorded, one can also produce an image of the source intensity around the detector using Compton imaging. A simple back-projection (SBP) image can be achieved by summing up the back-projection cones in the image space [1]. Maximum-likelihood deconvolution provides superior angular resolution by considering the probabilities that each measured event was produced by a photon originating from each direction in space [1,2].

Prior analysis did not include events that involve charge collection by adjacent pixels in the image reconstruction algorithm [1–5]. These events are defined as side-neighboring events and their probability of occurrence increases with gamma-ray energy. This work improves the Compton imaging efficiency by including side-neighboring events in the imaging reconstruction.

2. Charge-sharing events

In this work, we used a pixelated CdZnTe detector with dimensions of 2 cm × 2 cm × 1.5 cm. The anode of this detector

is divided into an 11 × 11 array of pixels with a pixel pitch of 1.72 mm. The lateral positions of the interaction are determined by the anode pixel that collects the electrons. The interaction depth is found by the electron drift time. The depth uncertainty is about 0.5 mm.

The electron cloud from a single gamma-ray interaction can be collected by and shared between several neighboring pixels. This phenomenon, known as charge-sharing, can be produced for several reasons: a large electron cloud has a size comparable to the pixel pitch; the electron cloud is located directly over the gap between pixels; the electron cloud diffuses while drifting towards the anode; and the X-ray emission from a photoelectric interaction. However, it is also expected that some side-neighbor events will occur due to two gamma-ray interactions in adjacent pixels. The two mechanisms for generating side-neighboring events are difficult to distinguish and prior work did not include the events in the Compton image reconstruction.

Theoretically, charge-sharing interactions should be combined into a single interaction because they are produced from a single electron cloud. However, it is very challenging to differentiate charge-sharing events from side-neighbor Compton scattering events. To identify that two interactions took place the separation distance between the interactions must be greater than the spatial resolution of the device. The spatial resolution of the ASIC readout system used in this work [6] is limited to the pixel pitch. Thus, it is impossible to differentiate multiple interactions from charge sharing in side-neighbor pixels based on the separation information within the plane of the pixels. The only remaining possibility is to separate charge-sharing events from multiple-interaction events based on the depth of interaction in each pixel.

* Corresponding author.
  E-mail address: wywang@umich.edu (W. Wang).

Table 1
The definition and the event fraction for each category of three-pixel side-neighbor events at 662 keV.

	Charge sharing	Compton scattering	Others
First interaction is involved in the side-neighboring pixels	Cat. 1: 22.4%	Cat. 2: 18.5%	Cat. 3: 5.2%
First interaction is not involved in the side-neighboring pixels	Cat. 4: 16.5%	Cat. 5: 25.7%	Cat. 6: 11.7%
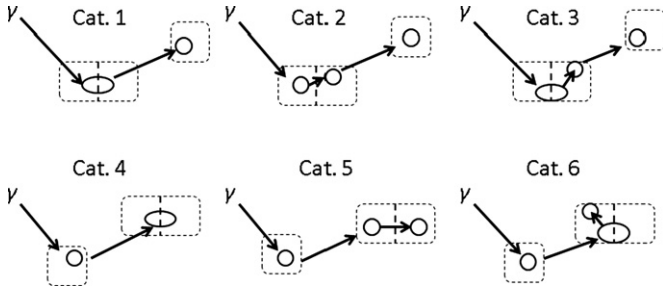
Fig. 1. Illustrations for each category in Table 1.

However, the average depth separation is shown in this work to be small relative to the depth resolution. Furthermore, the drift time measurement in a pixel may be distorted due to interference from the collection of a charge cloud in a neighboring pixel, further degrading the depth resolution of side-neighboring events.

Spatial resolution better than the pixel pitch, known as sub-pixel resolution, is achievable if the readout system can provide the charge induction as a function of time for each pixel. This has been achieved by sampling the preamplifier signal for each pixel at 80 MHz and analyzing the transient charge induction on the pixels that do not collect charge [7]. The capabilities of such a system will increase the probability of correctly identifying the number and the type of interactions as well as their respective locations.

The charge-sharing effect can be reduced by increasing the pixel pitch of the detector. However, increasing the pixel size will cause poorer energy resolution because it increases the position uncertainty, reduces the small pixel effect [8], and increases the leakage current collected by each pixel. As a consequence, the enlarged pixel size will improve the non-charge-sharing imaging efficiency while degrading the noise performance and angular resolution in the reconstructed image. With our current detector configuration, about 31% and 61% of the multiple-pixel events at 662 keV and 1333 keV
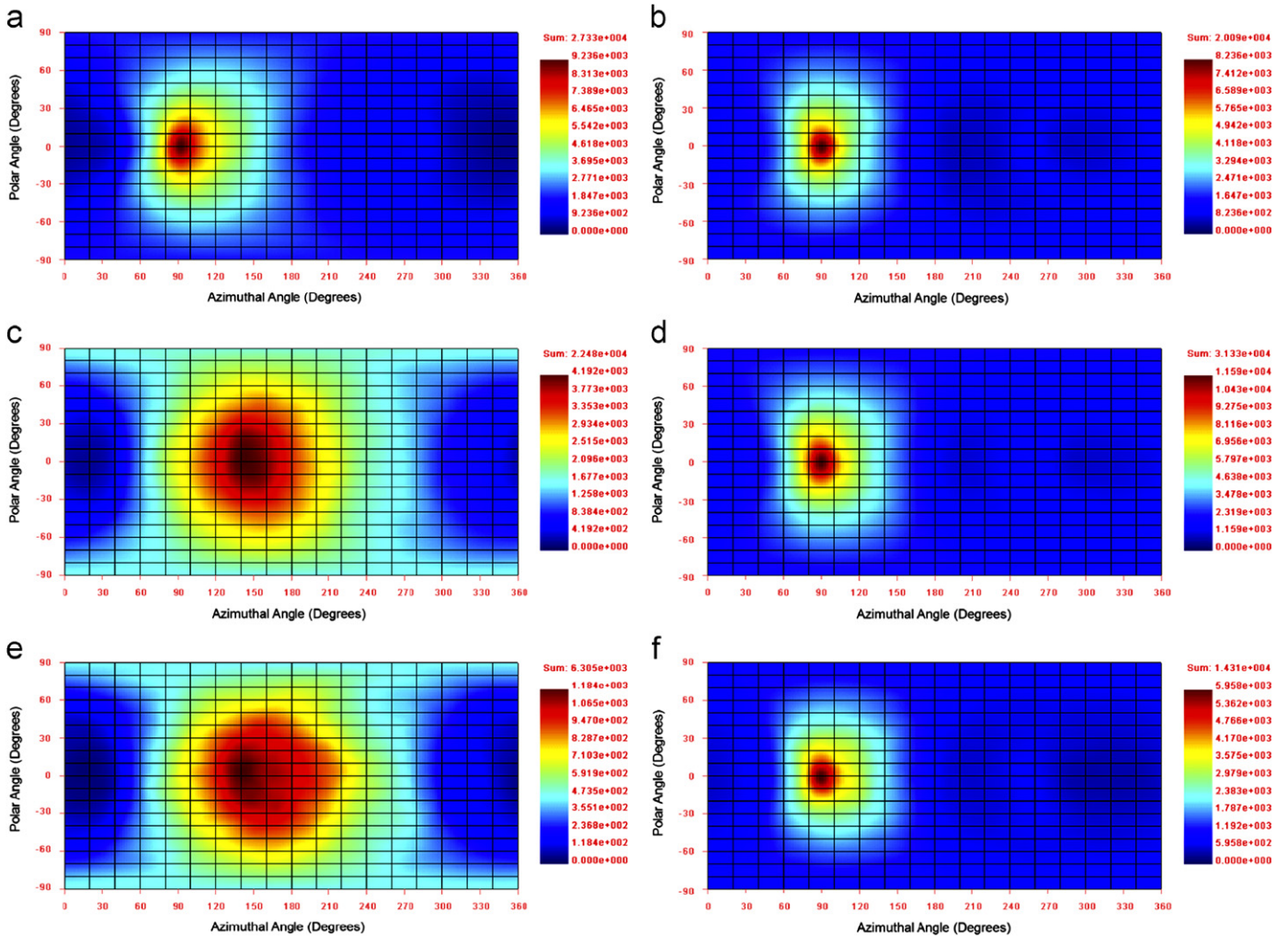
Fig. 2. All side-neighbor interactions are combined into a single interaction. The SBP image reconstruction is performed with these combined 2-interaction events (originally 3-pixel events) from six categories: (a) category 1; (b) category 4; (c) category 2; (d) category 5; (e) category 3; and (f) category 6.

are side-neighbor events, respectively. The following section separates the simulated side neighbor events into different categories, based on the type and the sequence of the interactions, and explores how to maximize the number of side-neighbor events that produce a correct source image. A method is then proposed and evaluated using the experimental data.

3. Side-neighbor events from simulated sources

Our group has developed a program to simulate the entire response of our system, from the generation, movement, and induction of charge to the readout process of our existing ASIC systems [9].

3.1. 662 keV

Using this software, we simulated the detector and the ASIC response from a point source that emits 662 keV photons. The simulation focused on events that trigger two adjacent pixels along with a third pixel that is spatially separated from the other two. These three-pixel events are divided into six categories based on the sequence and the type of interaction that produces the side-neighbor events, as shown in Table 1 and Fig. 1. We have

three possible options for each event: use the side-neighbor interactions in the image reconstruction without modification (assume that they are side-neighbor Compton events), combine side-neighbor interactions to one interaction (assume they are charge-sharing events), or exclude from the image reconstruction. Categories 1 and 4 are charge-sharing events, so the averaged depth and summed energy in the side-neighbor pixels should be input to the imaging algorithm as a single interaction. Categories 2 and 5 are three-interaction Compton events, so theoretically they should be only used in the image reconstruction directly. Categories 3 and 6 are the events that undergo both charge sharing and Compton scatter in the side-neighbor pixels.

In this work, we first combined all side-neighbor interactions by using the averaged depth and summed energy in each category, and performed image reconstruction with these new two-interaction non-side-neighbor events. We then directly reconstructed images from each category without combining side-neighbor events.

Fig. 2 shows the reconstructed image using the SBP algorithm after combining all side-neighbor events in each category. The averaged depth and summed energy in the side-neighbor pixels are input to the imaging algorithm as a single interaction. After combining side-neighbor interactions, as expected, categories 1 and 4 make correct images, while categories 2 and 3 make poor images that point
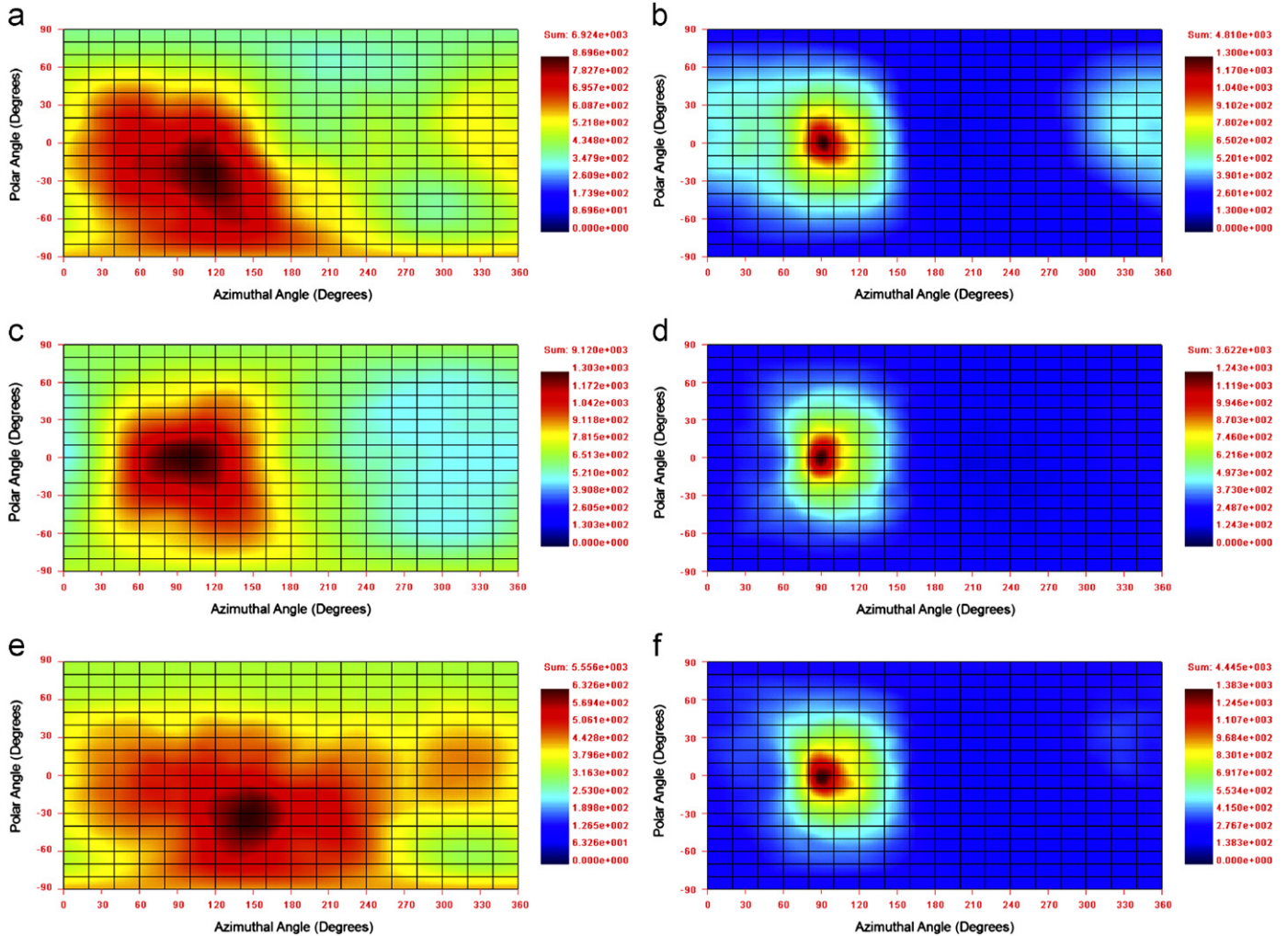

Fig. 3. The SBP image reconstruction is directly performed with three-pixel side-neighbor from all six categories. The events are from a simulated point source that emits 662 keV photons: (a) category 1; (b) category 4; (c) category 2; (d) category 5; (e) category 3; and (f) category 6.

to the wrong direction. The reconstructed image from category 4 has an angular full width at half maximum (FWHM) of 38.3°. In addition, categories 5 and 6 make hot spots centered at the source direction with angular FWHM of 42.8° and 45.2°, respectively. The first interaction in categories 5 and 6 is a Compton interaction collected by a single pixel with no neighboring pixels that collect charge. By combining the second and the third interactions, the cone angle remains unchanged because it is only dependent on the total energy

and the energy deposition of the first Compton scatter. Since the separation distance between the side-neighboring second and third interactions is small compared to the average separation distance between the first and the second interaction locations, the cone axis has a small change in both categories 5 and 6 after combining side-neighbor interactions. As a consequence, the full width at half maximum (FWHM) of the hot spot in Fig. 2(d) and (f) is 4.5° and 6.9° larger than Fig. 2(b), respectively.
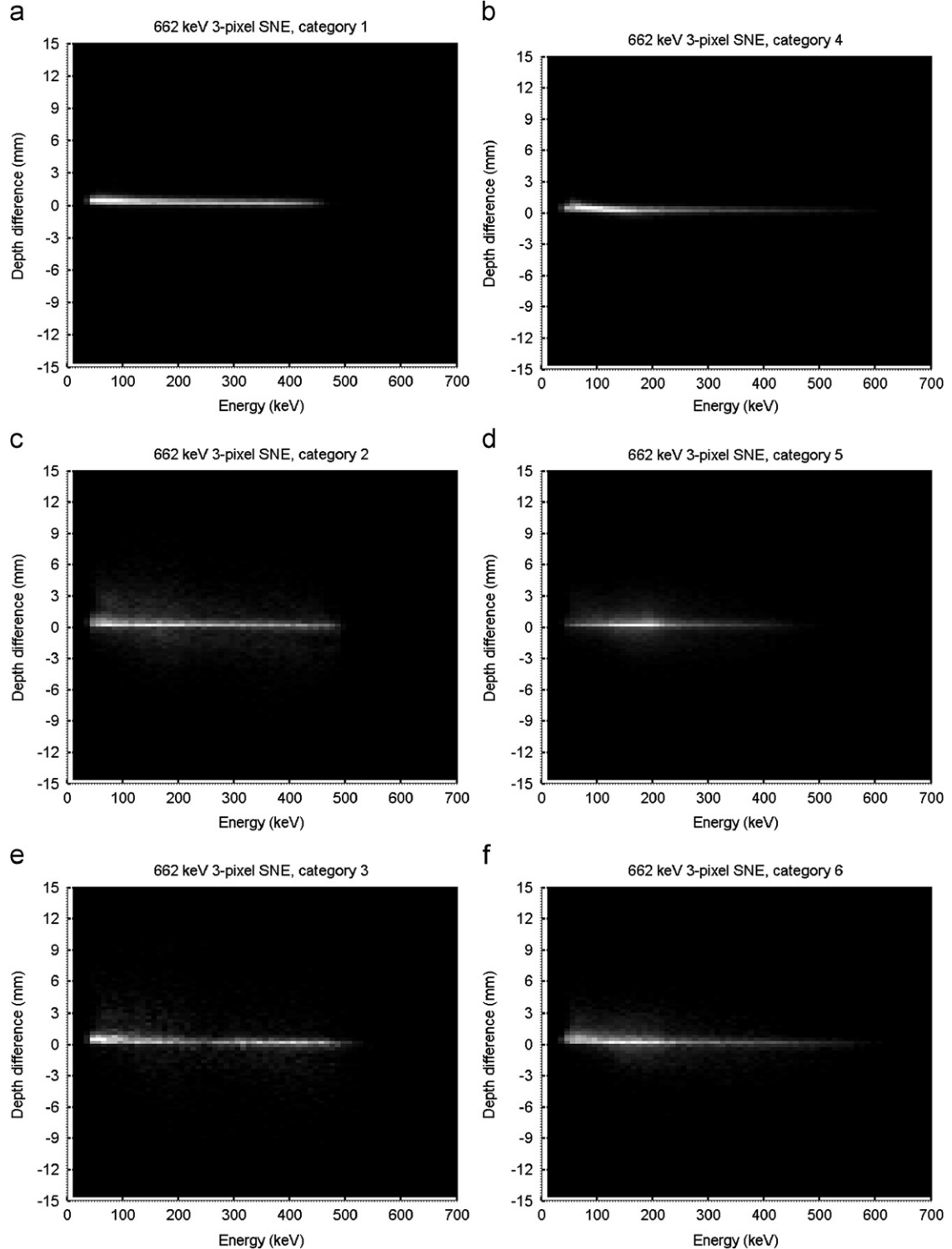

Fig. 4. The distribution of the depth difference between two side-neighbor interactions at 662 keV: (a) category 1; (b) category 4; (c) category 2; (d) category 5; (e) category 3; and (f) category 6.

The results of treating all six categories as three-interaction Compton events are shown in Fig. 3. In this case, only categories 4–6 reconstruct a single point source in the correct direction. In these three categories, the first interaction is a Compton scatter that does not involve one of the side-neighboring pixels. For the same reason described in the last paragraph, the reconstructed cone angles are correct in categories 4–6. In category 2, the side-neighbor events are from true Compton interactions. In principle, these events can be directly used in the imaging reconstruction. However, category 2 produces a very poor image due to the large cone-axis uncertainties associated with the short separation distance between the first and the second interaction occurring in side-neighboring pixels.

To summarize, category 1 can only produce a correct image after combining side-neighbor interactions. Categories 2 and 3 will never make a decent image and should be excluded from the image reconstruction. Finally, categories 4–6 can make a correct image whether or not side-neighbor interactions are combined. Ideally, the measurement system would be capable of separating these categories such that the appropriate action could be taken on an event-by-event basis.

The only parameters available to separate the six categories, given the readout system used in this work, are the energy and depth information recorded in each of the neighboring pixels. Fig. 4 shows the distribution of the depth difference between side-neighbor interactions as a function of the energy collected by each pixel for each category. No region can be drawn to clearly separate category 1 from category 4, category 2 from category 5, or category 3 from category 6. It is possible to differentiate categories 2 and 3 from category 1 such that events with large separation distances would be discarded. However, this would result in the loss of an approximately equal number of good events from categories 5 and 6. Therefore, in order to maximize the imaging efficiency, the best strategy for this readout system is to combine all side-neighbor events, as this provides the highest fraction of events that produce a correct image. From Table 1, this correctly combined fraction for three-pixel side-neighbor events at 662 keV is about 76.3%.

3.2. 1333 keV

A similar analysis was performed with a simulated point source which emits 1333 keV photons. The same conclusion can

Table 2
The definition and the event fraction for each category of three-pixel side-neighbor events at 1333 keV.

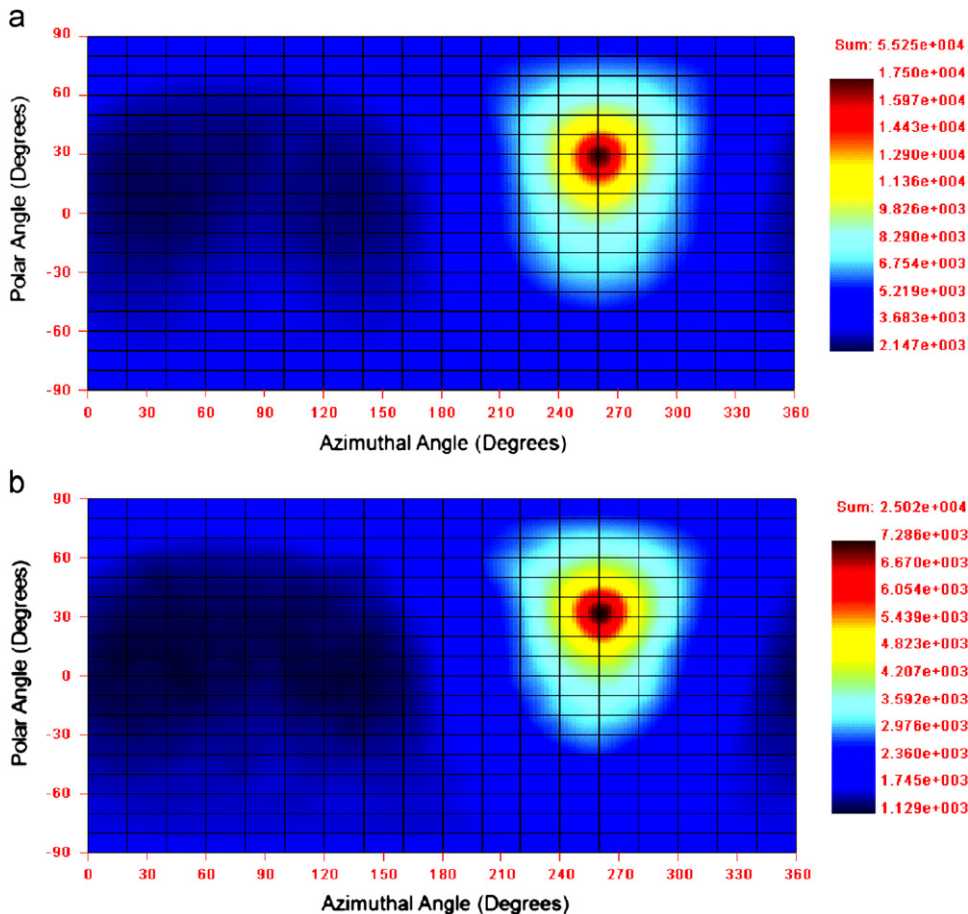|	Charge sharing	Compton scattering	Others
First interaction is involved in the side-neighboring pixels	Cat. 1: 44.8%	Cat. 2: 14.1%	Cat. 3: 9.4%
First interaction is not involved in the side-neighboring pixels	Cat. 4: 10.0%	Cat. 5: 13.5%	Cat. 6: 8.2%

Fig. 5. A SBP image with a Cs-137 source located at polar angle of 30° and azimuthal angle of 260° using two-, three- and four-interaction events. An energy window of 600 keV to 720 keV is used: (a) 55,252 non-side-neighbor events and (b) 25,023 side-neighbor events.
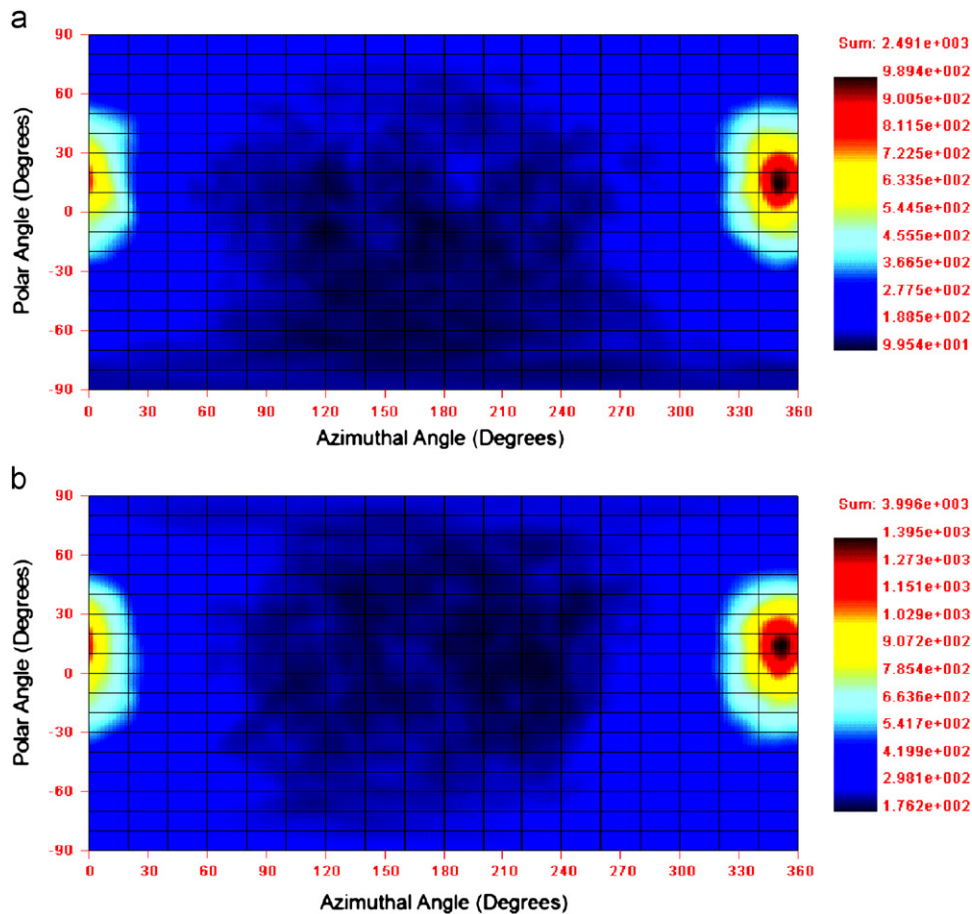
Fig. 6. A SBP image with a Co-60 source located at polar angle of 15° and azimuthal angle of 350° using two-, three- and four-interaction events. An energy window of 1250 keV to 1400 keV is used: (a) 2491 non-side-neighbor events and (b) 3996 side-neighbor events.

be drawn that the most effective way to use the side-neighbor events is to combine all side-neighbor interactions. From Table 2, about 76.5% of the combined three-pixel side-neighbor events are capable of producing a correct image.

All of these conclusions still hold for side-neighbor events with more than three triggered pixels as long as two or more unique interaction locations can be identified.

4. Performance verification with measurements

A Cs-137 and a Co-60 point source are measured separately. Fig. 5(b) shows the SBP image using only events that involved side-neighboring pixels. An energy window from 600 keV to 720 keV was used to image 25,023 two-, three-, and four-interaction events from the Cs-137 measurement. Fig. 5(b) has a similar image quality compared to Fig. 5(a) which uses 55,252 two-, three- and four-interaction non-side-neighbor events from the same measurement in the same energy window.

Fig. 6(b) shows the SBP image only using 3996 side-neighbor two-, three- and four-interaction events in energy window from 1250 keV to 1400 keV from the Co-60 measurement. Fig. 6(b) has a similar image quality compared to Fig. 6(a) which uses 2491 two-, three- and four-interaction non-side-neighbor events from the same measurement in the same energy window.

Thus, by combining all side-neighbor interactions, the imaging efficiency at 662 keV and 1333 keV is improved by 45% and 160%, respectively, with no observable degradation of the image quality.

5. Conclusion

Many charge-sharing interactions can be classified as a single interaction and used for Compton image reconstruction. The three-pixel side-neighbor photopeak events from a simulation were divided into six categories based on interaction type. Analysis of this simulation shows that the most effective strategy is to treat all side-neighbor events as charge-sharing events and to combine all side-neighbor interactions into a single interaction. By including these side-neighbor events in the Compton image reconstruction, we can still correctly reconstruct the source distribution using the experimental data and improve the imaging efficiency by about 45% and 160% for 662 keV and 1333 keV incident photons, respectively. About 76% of these combined events reconstruct rings that pass the source direction.

References

[1] D. Xu, Z. He, F. Zhang, 4π compton imaging with single 3D position sensitive CdZnTe detector, in: Proceedings of the SPIE, vol. 5540, pp. 144–155.

[2] C.E. Lehner, Z. He, F. Zhang, IEEE Transactions on Nuclear Science NS-51 (2004) 1618.
[3] D. Xu, Z. He, Nuclear Instruments and Methods in Physics Research Section A: Accelerators, Spectrometers, Detectors and Associated Equipment 574 (2007) 98.
[4] W. Wang, C.G. Wahl, Z. He, Maximum likelihood estimation maximization deconvolution in spatial and combined spatial-energy domains for combined single-, two- and three-interaction events, in: Nuclear Science Symposium Conference Record (NSS/MIC), IEEE, 2008.
[5] W. Wang, C. Wahl, J. Jaworski, Z. He, IEEE Transactions on Nuclear Science NS-59 (2012) 469.
[6] F. Zhang, Z. He, IEEE Transactions on Nuclear Science NS-53 (2006) 3021.
[7] Y. Zhu, S.E. Anderson, Z. He, IEEE Transactions on Nuclear Science NS-58 (2011) 1400.
[8] H.H. Barrett, J.D. Eskin, H.B. Barber, Physical Review Letters 75 (1995) 156.
[9] J.C. Kim, S.E. Anderson, W. Kaye, F. Zhang, Y. Zhu, S.J. Kaye, Z. He, Nuclear Instruments and Methods in Physics Research Section A: Accelerators, Spectrometers, Detectors and Associated Equipment 654 (2011) 233.